Environ Earth Sci (2011) 63:251–261
DOI 10.1007/s12665-010-0696-y

ORIGINAL ARTICLE

Induced polarization, resistivity, and self-potential: a case history of contamination evaluation due to landfill leakage

José Domingos Faraco Gallas · Fabio Taioli · Walter Malagutti Filho

Received: 24 March 2009 / Accepted: 8 August 2010 / Published online: 17 August 2010

Abstract This article compares the efficiency of induced polarization (IP) and resistivity in characterizing a contamination plume due to landfill leakage in a typical tropical environment. The resistivity survey revealed denser electrical current flow that induced lower resistivity values due to the high ionic content. The increased ionic concentration diminished the distance of the ionic charges close to the membrane, causing a decrease in the IP phenomena. In addition, the self-potential (SP) method was used to characterize the preferential flow direction of the area. The SP method proved to be effective at determining the flow direction; it is also fast and economical. In this study, the resistivity results were better correlated with the presence of contamination (lower resistivity) than the IP (lower chargeability) data.

Keywords Resistivity · Induced polarization · Self-potential · Environmental geophysics

J. D. F. Gallas (✉) · F. Taioli
Geosciences Institute, University of São Paulo,
Rua Do Lago, 562, São Paulo, SP 05508-080, Brazil
e-mail: jgallas@usp.br

F. Taioli
e-mail: ftaioli@usp.br

W. Malagutti Filho
Institute of Geosciences and Exact Sciences,
São Paulo State University, Campus Bela Vista,
PO Box 178, Rio Claro, SP 13506-900, Brazil
e-mail: malaguti@rc.unesp.br

Introduction

In the last few years, applied geophysics has increased its applications in the fields of environmental assessment and hydrogeology. This study describes the application of three geophysical methods to assess a typical environmental problem in a tropical region: resistivity, induced polarization (IP), and self-potential (SP).

The selected test area lies next to the Alvarenga dump, which is located in the São Bernardo do Campo municipality in São Paulo State, Brazil. Alvarenga dump began operation in 1972 and received about 2 million metric tons of domestic rubbish until its closure in 2001. The pollution can be easily noted by the color and smell of the water. The surveyed location is a swampy area located downstream from the dump. Further downstream is the Billings Reservoir, which receives all of the leakage that is carried by the spring and ground water that crosses the study area. Figures 1 and 2 present a sketch of the study area with the location of the geophysical survey.

The objectives of this study were to establish the lateral limits of the contamination plume, to determine the plume's depth and preferential flow directions, and to compare the efficacy of resistivity and IP methods in characterizing the plume. The results obtained from the resistivity and IP surveys were compared considering both the efficacy and the viability of applications of IP in a situation diverse from its historical use (i.e., mineral prospecting).

Geology of the Alvarenga dump area

In the study area, the groundwater is very shallow, always with depths ≤ 1 m, and in places it reaches the surface. The

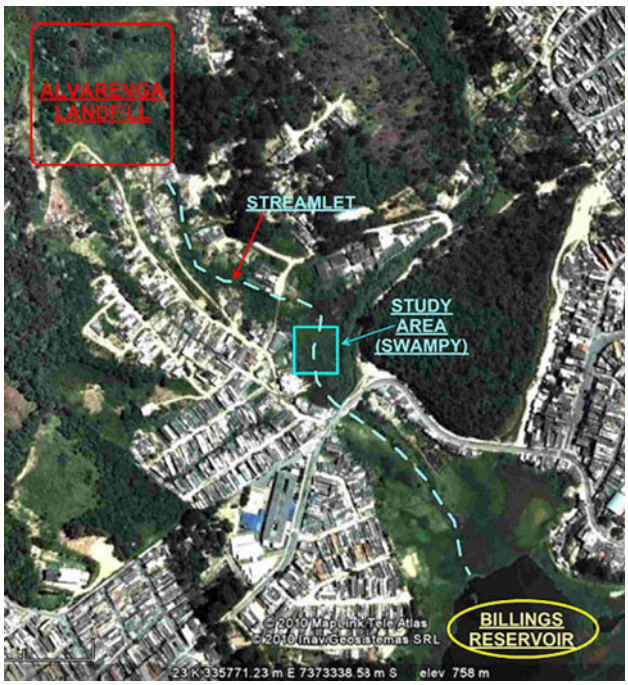

Fig. 1 Study area

local soil is the weathering product of low-grade metamorphic rocks (schist and shale), which represent the basement of the area. The schists are micaceous or quartzose and exhibit predominantly medium- to fine-grained crystals and well-developed foliation. These rocks normally present a thick weathering mantle (weathered soil and regolith) of 10 m in plains and a few meters more in steeper relief. The weathered soil is composed of silty clay in the areas with micaceous schist and silty sand in the areas with quartzose schist, and it is 2–3 m thick. The shale is very fine-grained, has well-developed foliation, and contains quartz and sericite. Its weathered soil is normally silty, and is about 1 m thick. Otherwise, the weathering mantle is very deep and can reach about 20 m in moderate relief and around 1 m in the steepest areas. The aquifer system is typical of crystalline rocks, with water flowing through the fractures except in the weathered area, where the soil is permeable and has high transmissivity.

Methodology

The dipole–dipole array was used in the IP-resistivity survey. The distance between electrodes was AB = MN = 5 m with five levels of investigation. The distance between the surveyed sections was normally 10 m. The survey was performed parallel and perpendicular to existing drainage. The dipole–dipole array was chosen because it is a symmetrical array that provides good quality information in both horizontal and vertical directions. This is in accordance with Ward (1990) and Gallas (2000), who analyzed the performance of different arrays in terms of lateral and vertical resolution. The SP measurements were taken on an array of 5 × 5 m using the potential technique (i.e., using one electrode as a base and walking with the other). The data from the three surveys were integrated and then analyzed. The extension of the dipole–dipole sections and the SP measurement points are shown in Fig. 2.

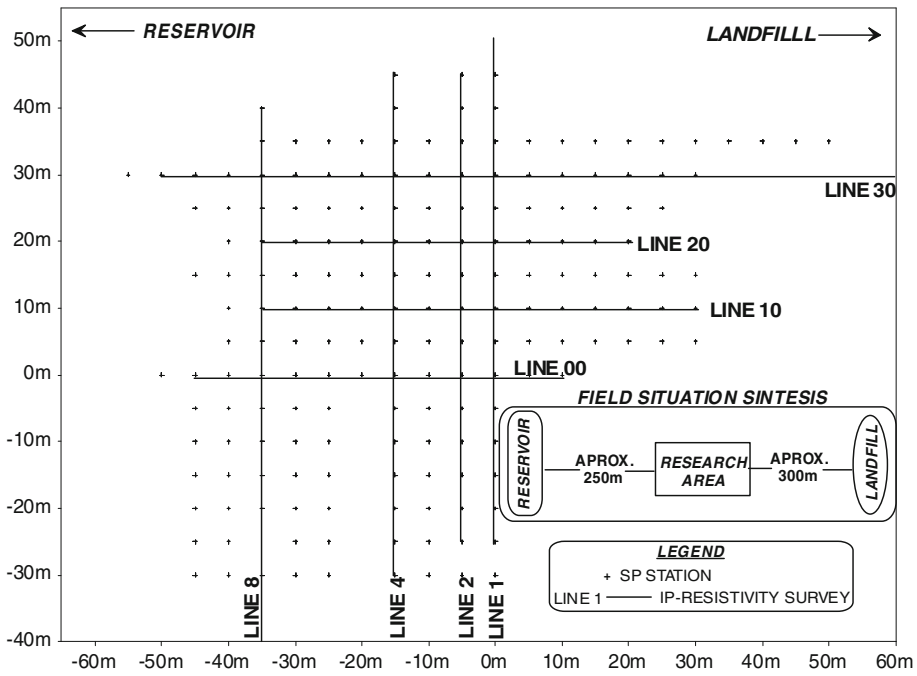

Fig. 2 Extension of the dipole–dipole sections and the SP measurement points

The instrumentation used was composed of a receptor (IPR-10A) and a transmitter (TSQ3-3kW), both produced by Scintrex, and it was suitable for taking IP, resistivity, and SP measurements. This paper presents the IP and resistivity data in the form of pseudo sections and modeled sections. In pseudo sections, the assumed forms and contours are not true, but rather an approximation. Pseudo sections do not depend exclusively of the measured resistivity distribution, but also involve the electrode geometry configuration used (e.g., pole–pole, pole–dipole, dipole–dipole). The resistivities and chargeabilities calculated are referred to as apparent values because they represent a resulting value of the chargeabilities and resistivities of a sub-surface volume. The depth reached by the survey also depends on the resistivities of the materials and the geometry of the electrode array used.

To obtain a "real" section, an inversion process must be performed. The inversion processes, theoretically, allow researchers to obtain reasonable models for the geological structures being studied. An automatic 2D (bi-dimensional) inversion process was used in this study to establish a model of the probable real resistivity distribution and to eliminate the distortions caused by the electrode array. The raw IP-resistivity pseudo section data were processed using the software RES2DINV (Geotomo Software 2004) and Surfer 8 (manufactured by Golden Software). The first is specific for inversion of resistivity and IP data, and the second is generally used to interpolate spatial data. The results of the inversion process were exported as XYZ data and then interpolated with the aim of improving visualization of the data.

RES2DINV uses a fast and efficient technique for data inversion that was developed by Loke and Barker (1996a, b) and deGroot-Hedlin and Constable (1990). It is based on the least square and the smoothness-constrained methods. Theoretically, it provides a 2D subsurface model free of the distortions presented in the pseudo sections and those due to the electrode array used. The 2D modeling system of the software divides the subsurface into rectangular blocks, and the values of resistivity and chargeability for each block are calculated and related to the measurement points assumed in the pseudo section. The optimization method reduces the difference between the measured and the calculated values and adjusts the values for each block. The distribution and size of the blocks are generated automatically by the software in such a way that the block number does not exceed the number of measured points (except when the user imposes this criterion). The final depths of the blocks (i.e., the depths of the investigation levels calculated) are approximately those proposed by Edwards (1977) for the largest distance of the electrode array. It is about half of the depth value proposed by Hallof (1957) for pseudo sections. The user may also adjust these depths if direct information is available.

The IP-resistivity pseudo section data were processed using the software RES2DINV (Geotomo Software 2004) that produces a modeled section intended to minimize the distortions present in conventional representations (Hallof 1957). The modeled sections are the product of an automatic 2D inversion process based on finite element and finite difference techniques (Loke and Barker 1996a, b). This process aims in calculating the real sub-surface resistivity distribution. Eventual distortions in the pseudo sections that are inherent in the electrode array are minimized in this process.

The SP method was used to determine the preferential flow directions of the sub-surface fluids in the contaminated area. The distance between measurements was 5×5 m in both directions. The field survey was conducted using two non-polarizable electrodes (Cu in $CuSO_4$ solution), one millivoltmeter and wires. The potential measurement technique was used, meaning that one of the electrodes was kept fixed at a base station and the other was moved to the points of measurement. This survey method is less affected by noise or measurement errors than the gradient technique (i.e., when the two electrodes are moved simultaneously).

Discussion of resistivity

Electrical conduction can be either ionic or electronic. In nature, ionic conduction predominates, thus it is the most significant mode in resistivity studies. The correlation between the resistivity and underground contamination is related the concentration of ions: In contaminated areas, the resistivity is lower because contamination is associated with a greater concentration of ions. Thus, contaminated areas are characterized by better propagation of the current, which results in zones with lower resistivity. This behavior follows Ohm′s law (Eq. 1):

$$\vec{J} = \sigma \vec{E} \tag{1}$$

or

$$\vec{E} = \rho \vec{J}$$

where J is the current density, σ is the conductivity of the medium, E is the electric field, and ρ is the resistivity or the free charge quantity.

Ionic conduction is the most important factor when prospecting underground using resistivity. Because most rocks and underground conditions are poor conductors, their resistivities should be extremely high. However, due to the electrolytes present in the pore space, this is not

always true. When considering this factor, this medium behaves as an electrolytic conductor (Telford et al. 1990). Resistivitiy also varies with the mobility, concentration and degree of ionic dissolution and this degree depends on the dielectric constant of the solution. In comparison with the electronic conduction, ionic conduction is slower and represents a material transport. Therefore, in most lithologies, conduction is electrolytic and the conductor is a solution of water and mineral salts distributed in a complex way in the pores of the rock. The resistivity depends on the quantity of water, its salinity, and the way the water is distributed in the rock.

When a salt is in solution in water, the ions are freely dissociated. When an electric field is applied, the cations accelerate towards the negative pole and the anions accelerate to the positive pole. At the same time, the velocity of the ions is decreased due to the viscosity of the solution. In an aqueous solution, the time an ion takes to reach its final velocity is <1 ms and this final velocity is defined as ion mobility. In other words, the ion mobility is the ion velocity when a potential gradient of 1 V/m is applied, and its dimension is in meter per second (Keller and Frischknecht 1977). Ion mobility depends on ion concentration and temperature. As the electrolyte temperature increases, the viscosity decreases, allowing a higher final velocity for the same potential gradient. If the solution is rich in ions, the dislocation of an ion affects the dislocation of other ions present in the solution and leads to reduction in the final velocity. A rock's resistivity decreases with increased water content and also with the volume of dissolved chloride, sulfate, and other salts and minerals. Another condition that enables good electrical conduction is when the pores are interconnected and filled with water.

When trying to correlate resistivity with water content in rocks, Archie (1942) observed that the resistivity varies approximately with the inverse of the square of the porosity when the rock is saturated with water. That observation led to the empirical relation between resistivity and porosity known as Archie's law (Eq. 2).

$$\rho = a\rho_{\mathrm{w}}\varphi^{-m} \tag{2}$$

where ρ is the total resistivity, ρ_{w} is the resistivity of the pore water, φ is the porosity and a and m vary depending on the porosity type and degree of cementation, respectively.

Discussion of IP

Despite common use in mineral prospecting, IP has not been used much to assess engineering and groundwater problems (Roy and Elliot 1980). It may be useful for such studies, as well as for environmental studies. IP is an electrical phenomenon caused by current transmission in the soil. It is observed as an out-phased voltage response. As a geophysical measurement, IP is related to a resistive block or to an electrical polarization of the earth materials, which is stronger in the pores filled with fluids and in neighboring metallic minerals. Therefore, the IP phenomenon is more observable in rocks rich in metallic minerals. The main advantage of the IP method is its capacity, in favorable conditions, to detect the presence of metallic minerals. Even concentrations as low as 0.5% sulfide may be identified by IP (Sumner 1976).

Whenever a potential difference (ΔV) is established (due to the current flow in the soil), this potential does not reach the final value (i.e., the maximum potential generated by the current applied), neither when applied nor when the current application is discontinued. Actually, IP describes a curve, $\Delta V_{\mathrm{IP}} = f(t)$, which links the asymptote ΔVp to the asymptote zero after interrupting the current injection (Fig. 3). This phenomenon is called IP (Bertin and Loeb 1976).

The quantity that characterizes the IP phenomenon is the area below the discharge curve, including the asymptote part, which tends to zero and is given by Eq. 3.

$$\mathrm{IP} = \mathrm{Area} = \int_0^{\infty} \Delta V_{\mathrm{IP}(t)}\mathrm{d}t \tag{3}$$

Actually, for practical reasons, IP is considered to be the potential in the time interval between t_1 and t_2 normalized by the primary voltage ΔVp. The quantity measured is expressed by Eq. 4 and is called apparent chargeability M.

$$\mathrm{IP} = M = \frac{1}{\Delta Vp}\int_{t1}^{t2} \Delta V_{(\mathrm{IP}(t)}\mathrm{d}t \tag{4}$$

The two main phenomena that might explain IP are metallic (or electronic) polarization (typical of metallic sulfides) and electrolytic polarization (typically non-metallic or due to membrane effects, such as in clays).

Normally, the current propagates through the soil via ionic conduction and metallic conduction. An electrochemical reaction occurs at the interface between the solids and the liquid, and this reaction is responsible for the

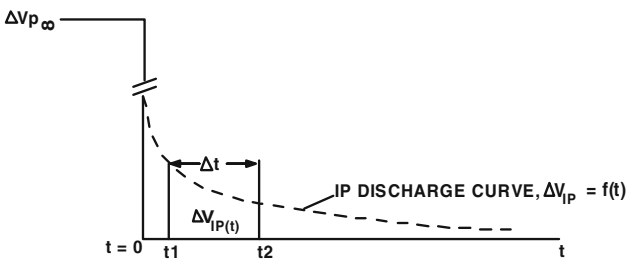

Fig. 3 IP discharge curve

transference of electricity between the ions in the solution and the free electrons in the metallic minerals. Several possible reactions are discussed in the literature (Klein and Shuey 1978a, b), but the predominant type of reaction in situ IP measurements is unknown.

The model established by Cole and Cole (1941) describes the IP phenomenon using a model in which a very simple electrical circuit simulates the ways the current flows at an interface and such a model can be applied for both metallic polarization and electrolytic membranes (Ward 1990). For metallic polarization, during current transmission the ions accumulate at the interface between the electrolyte and the metal and restrict the current flow until the equilibrium is re-established, as increased voltage is created at the interface. This situation is equivalent to what occurs with electrical dipoles. Whenever the current is interrupted, the ions slowly flow in the electrolytic environment to return to the initial equilibrium, and the residual voltage accumulated at the interface decreases, resulting in the IP effect (Bertin and Loeb 1976).

Clays are characterized by the very small size of their crystals, which are much smaller than those of other minerals. This means that clays have a greater surface-to-volume ratio and consequently the electrification of this surface has a higher effect on the macroscopic properties of these minerals. Cation exchange capacity is the most important property related to the IP effect in clays. Although difficult to measure, anion exchange also occurs, principally, it is believed, at the axis of rupture of the silicate layers; this is electrically analogous to the IP effect on the surface of other minerals.

Membrane polarization occurs in the soil where clay minerals partially obstruct the pores and consequently the free flow of ionic solutions. The diffuse cloud of cations (double layer) around the external surface of the particles is characteristic of clay-electrolyte systems. When a potential is applied, the positive charges pass through the cloud of cations while the negative charges accumulate, thereby producing an ion-selective membrane. Consequently, zones with high ion concentration form and a polarization membrane appears. The gradients of ion concentration formed are opposite to the current flow and reduce the current's mobility, which results in a polarization effect. This polarization is partially a function of the different mobility of cations and anions (Bertin and Loeb 1976; Sumner 1976).

Most of the charges adsorbed and adjacent to the membrane are located at the distance d from its surface (Grahame 1947):

$$d = \frac{K_e kT}{(2ne^2v^2)^{1/2}} \tag{5}$$

where n normal ion concentration in the electrolyte, v ion valence, e elementary charge, K_e relative dielectric permissivity of the fluid, k Boltzman's constant (1,38054 $\times$ 10^{-16} Erg/^{o}K), T temperature.

Therefore, the IP phenomenon becomes more intense with the increase of d:

$$IP \propto d \tag{6}$$

Equation 5 shows that d decreases when the ionic content, n, increases. Because contaminated areas have a higher ionic concentration, and IP is inversely proportional to the d parameter and to ionic concentration, these areas exhibit a lower IP value than non-contaminated areas (Eqs. 5, 6). In environmental studies of areas such as contamination plumes, landfills, and toxic fluids, changes in d might occur, which would make it possible to map the contamination, using detectable IP anomalies.

Discussion of SP

When studying contamination, one has to consider the flow potentials that are generated by the movement of underground fluids; this process commonly is called electrofiltration or electrokinesis. The movement of an electrolyte through a porous membrane produces a potential difference between the two sides of the membrane. If the underground material porosity is considered to be a capillary net through which groundwater percolates, the underground material also can be considered to be a membrane. The anions are absorbed by the capillary walls and attract the cations, thereby establishing an electrical double layer. The anions remain fixed while cations are moved through the capillary by the fluid flow, which creates a concentration of cations (Orellana 1972). These anomalous concentrations create a potential difference between the initial and final points that obey Helmholtz's equation (Eq. 7):

$$\Delta V = \frac{\xi \varepsilon P}{\eta \sigma} \tag{7}$$

where ζ potential difference at the double layer, ε dielectric constant, σ conductivity, η electrolyte viscosity, P water head between the extremes of the capillary (responsible for the electrolyte movement).

Natural potentials occur in nature due to several factors besides flow potentials, including redox potential differences and diffusion potentials. However, in our study, considering the low depth of the water level, the SP is due mainly to the flow potential.

For engineering and environmental studies, the SP method is applicable for determining the groundwater flow. SP anomalies are generated by the flow of fluids, heat, or ions in the subsurface, and the study of these anomalies has been useful for locating and delineating such flow and its associated sources (Gallas and Malagutti Filho 2001). The

main advantages of the SP method are its operational and instrumental simplicity and, consequently, the low cost. To conduct a SP survey, one only needs two non-polarized electrodes (e.g. Cu in a $CuSO_4$ solution in a porous recipient), one millivoltmeter, and isolated wires to connect the electrodes to the millivoltmeter.

In this study, the SP data were acquired using the potential technique, in which one of the electrodes is kept fixed at a base point and the other electrodes is moved to each of the measurement points. The potentials increase in the flow direction, and the amplitude of the flow is proportional to the hydraulic gradient. This means that the flow direction is from the lower to the higher potential. Therefore, a map with SP isopotential lines may indicate the spatial configuration, the direction, and the intensity of the flow.

Previous works

Contamination due to domestic rubbish may increase the concentration of some ions (mainly Cl^- and NO_3^-) in the groundwater (Varnier and Hirata 2002). In particular, the concentration of the chloride ion correlates with electrical conductivity and causes conductive plumes that may be mapped using geophysical methods, such as resistivity and ground penetrating radar (Nascimento et al. 1999). Seaton and Burbey (2002) compared dipole–dipole, Wenner, Wenner-Schlumberger, and pole–pole arrays using a 25 electrode system with three different spacings (2, 6, and 10 m) at a site with shallow soil depth (<20 m). The authors compared the inverted field data and numerical models simulating the structures present in the site and concluded that the dipole–dipole array provided more detail and depth than the Wenner or Wenner-Schlumberger arrays.

Ogilvy et al. (2002) applied resistivity to conduct a 2D survey using a series of parallel profiles aimed at mapping the spatial distribution of garbage and its leachate in an abandoned landfill. The authors use the term electrical resistivity tomography to designate the technique used. They used a pole–dipole array (distance between electrodes of 10 m and 8 investigation levels). To increase the data density and the lateral resolution, the distance between the measurement points was 5 m. They took measurements in both directions from the profiles that were spaced 10 m from each other. Elis (1999) used geophysical methods to study several landfills and concluded that resistivity is the best method when compared with SP and IP. Soupios et al. (2007) described the use of resistivity and the modeling of the data. They applied resistivity, electromagnetics (EM-31 and VLF), and the refraction seismic method to characterize a domestic disposal landfill on Crete Island. They suggested that the use of different techniques allows for the resolution of discrepancies, and they reported that resistivity provided the best results.

Silva (2003) applied a resistivity profiling survey (dipole–dipole array with electrode separation of 2 m), electromagnetics (EM-31), and SP in an area contaminated by domestic rubbish. Low resistivity and high conductivity values were associated with the contamination plume, and the SP survey showed the preferential flow direction. Vega de la et al. (2003) combined dipole–dipole and Wenner arrays to study a contamination plume of gasoline. They inverted the data of both arrays together and obtained satisfactory results in terms of investigation depth, thanks to the Wenner array and good horizontal resolution due to the dipole–dipole array. Godio and Naldi (2003) used 2D resistivity profiling to study a hydrocarbon contaminated area. They adopted a Wenner array with dipoles of 1 m because of the intense environmental noise.

Results

Figures 4 and 5 present the resistivity and IP pseudo sections and modeled sections, respectively. The pseudo sections present the raw data following the procedure proposed by Hallof (1957). The modeled sections present the resistivity and IP data after inversion. All eight studied profiles exhibited similar results, and only two sections (lines 8 and 30) are shown here due to space limitations. These profiles are located within the limits of the studied area. Line 8 is perpendicular to the drainage and the line 30 is parallel to it (Fig. 2). The results presented in Figs. 4 and 5 show all resistivity and chargeability values measured and modeled for those two lines.

The processing by RES2DINV considered 17 and 24 electrodes (lines 8 and 30, respectively) and resulted in a model of five strata. However, the way in which the modeled sections are presented indicates that the strata are plane parallel and that the data can be classified into two groups: contaminated and not contaminated. The data inversion was carried out for IP and resistivity simultaneously, and the root mean squares of the errors were 3.4 and 1.7% for chargeability (lines 8 and 30, respectively) and 18.3 and 14% for resistivity (lines 8 and 30, respectively) after five processing iterations. The results obtained from the inversion were interpolated by kriging using Surfer software.

To obtain a global picture of the resistivity and chargeability distributions in the area surveyed, it is possible to draw maps using the modeled data and by electing a specific investigation level with data taken from all of the sections surveyed. The choice of the most appropriate level is made by analyzing all data. If the

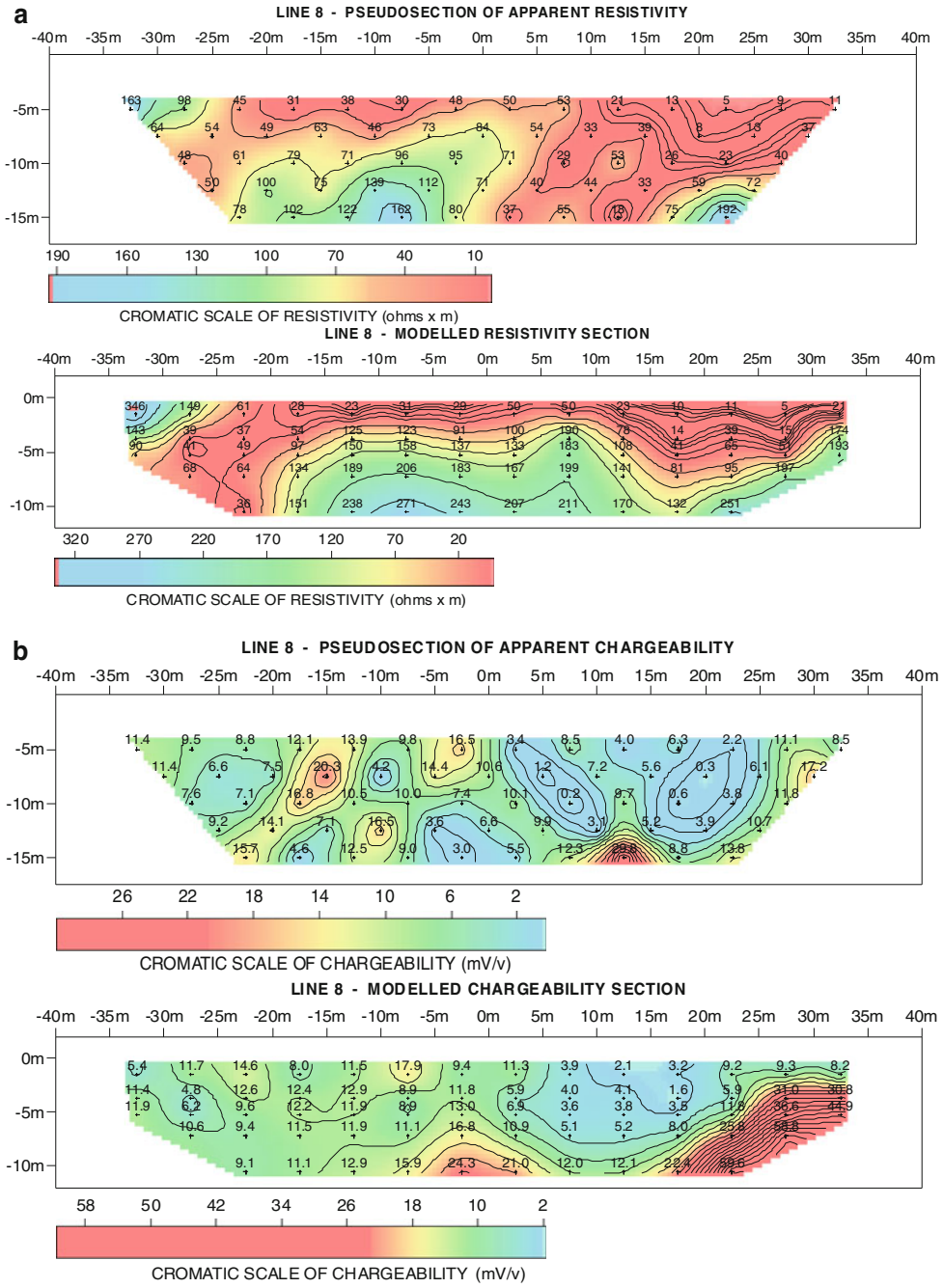

Fig. 4 **a** Pseudo section and modeled resistivity sections, line 8. **b** Pseudo section and modeled chargeability sections, line 8

dipole size was appropriate, the target is normally reached at the second investigation level and, normally, this is the most representative level (Gallas 2000; Gallas et al. 2003). If there is interest in analyzing the behavior of the contaminant with depth, it is possible to elect another level, and normally the fourth one is appropriate (Gallas 2000; Gallas et al. 2003). Another way to enhance this visualization is to use tridimensional simulation was done in the current study.

Figure 6 presents the 3D simulation of the modeled resistivity at level 2 of the dipole–dipole and shows that the zones with lower values of resistivity are related to the areas more affected by the contamination plume. Figures 7 and 8 present the 3D simulation of the modeled resistivity at levels 4 and 5 of the dipole–dipole and show that the resistivity is higher in these levels, which indicates that the contamination is less severe at greater depths. These figures also show that a region with low resistivity values appears downstream, which could indicate that the contamination may reach this level in that region.

Figures 9, 10, and 11 present the 3D simulation of the modeled chargeability of levels 2, 4, and 5 of the dipole–

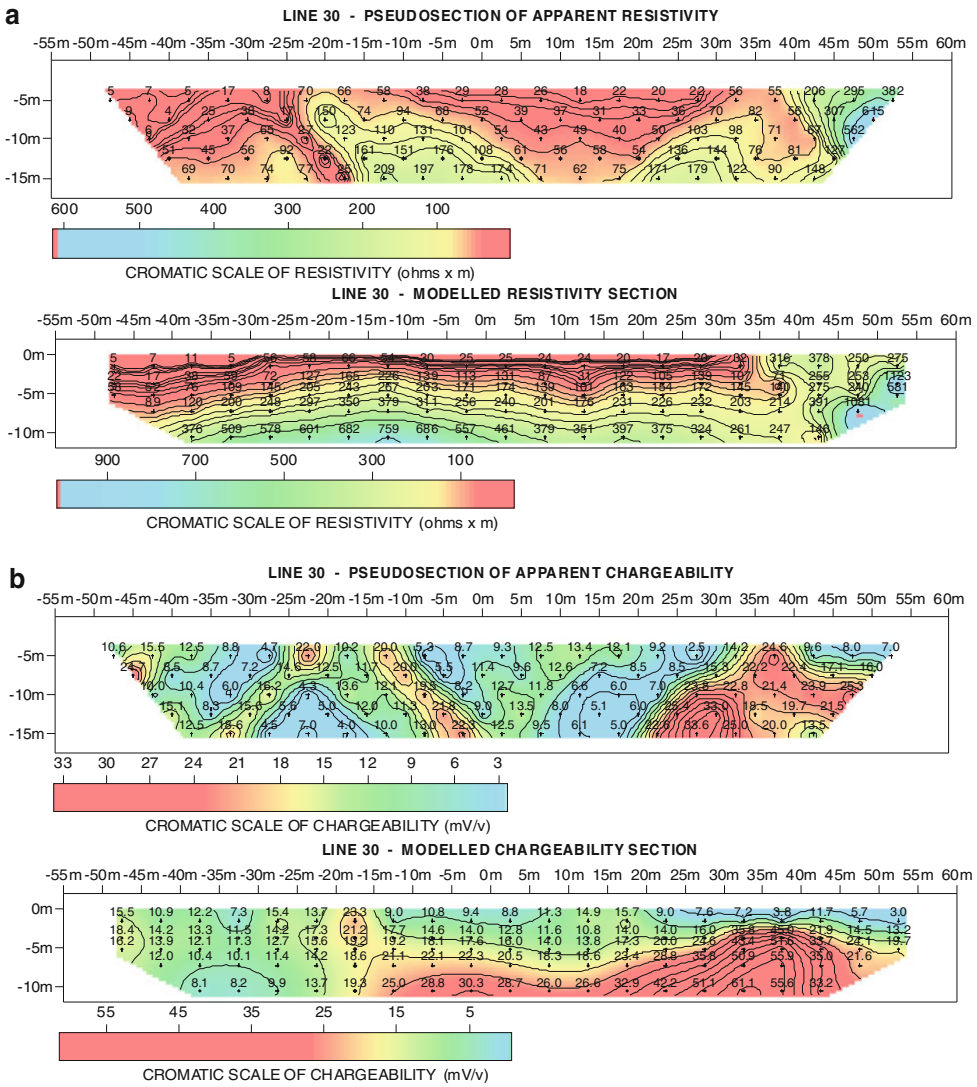

Fig. 5 **a** Pseudo section and modeled resistivity sections, line 30. **b** Pseudo section and modeled chargeability sections, line 30

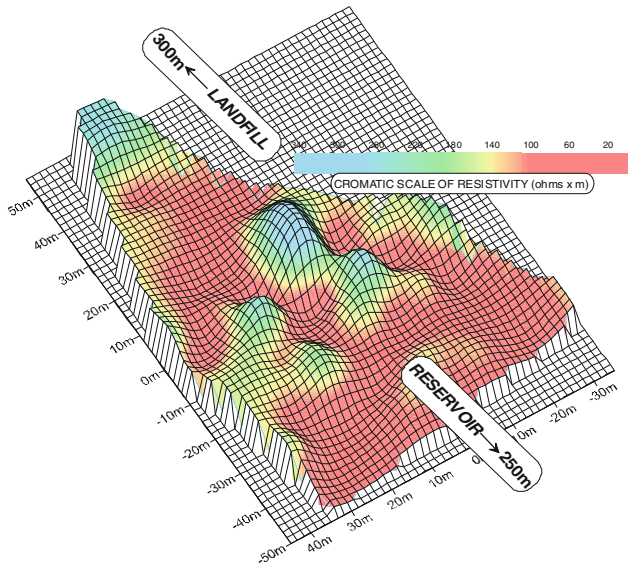

Fig. 6 3D simulation of the modeled resistivity at level 2 of the dipole–dipole

dipole. They show behavior similar to that presented by the resistivity data. Lower chargeability correlates to lower depths where the contamination is more severe. The 3D simulation presented in Fig. 9 (data from level 2), when compared with the 3D simulations shown in Figs. 10 and 11 (data from levels 4 and 5, respectively), shows that the IP phenomenon intensity is inversely proportional to the ion content, according Eqs. 5 and 6.

Figures 6, 7, 8, 9, 10, 11 are designated as simulations because they are not real 3D representations; instead they are 2D data distributions in a surface that changes proportionally with the oscillations of the values. Therefore, it is possible to observe that the pollutant presence (higher ionic content) implies a lower chargeability pattern in the IP section. It is unlikely that the low values of both chargeability and resistivity are due to causes other than the contamination. The water level in all areas is very shallow (<0.5 m). In addition, the contamination of the water can be sensed by its color and smell.

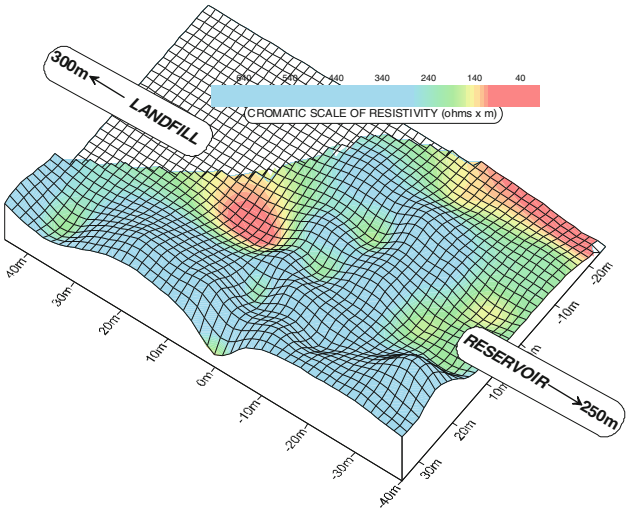

Fig. 7 3D simulation of the modeled resistivity at level 4 of the dipole–dipole

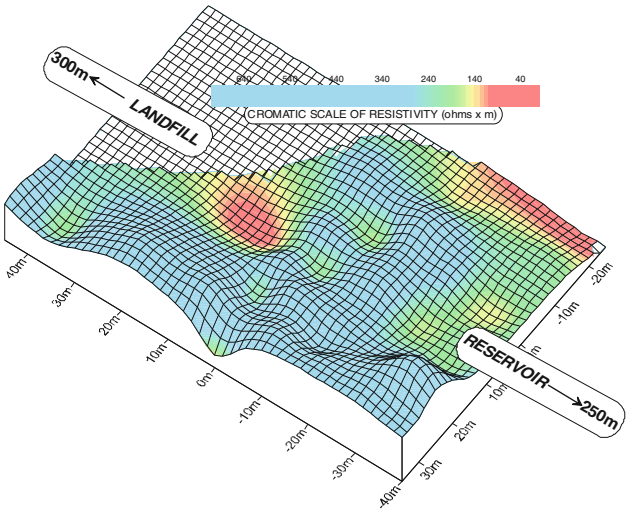

Fig. 8 3D simulation of the modeled resistivity at level 5 of the dipole–dipole

The flow potentials (also called electrofiltration or electrokinesis) are generated by the underground fluid movement and, in situations such as this (i.e., low depth of the groundwater) are the main cause of the natural electric potentials. The SP anomalies caused by such flow are very suitable for delineating the flow direction and the associated sources. Considering that the SPs are caused by the fluid flow, the potentials increase from upstream to downstream and the intensities are proportional to the hydraulic gradient. Therefore, the flow direction is from the lower to the higher potential and the equipotential map shows the preferential flow directions. Figure 12 presents the SP results and indicates that the preferential flow direction is from the landfill to the reservoir. The figure also shows a differentiation in the central part of the map.

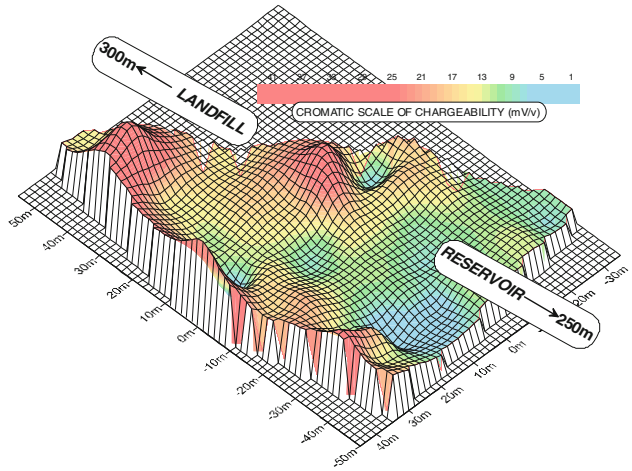

Fig. 9 3D simulation of the modeled chargeability at level 2 of the dipole–dipole

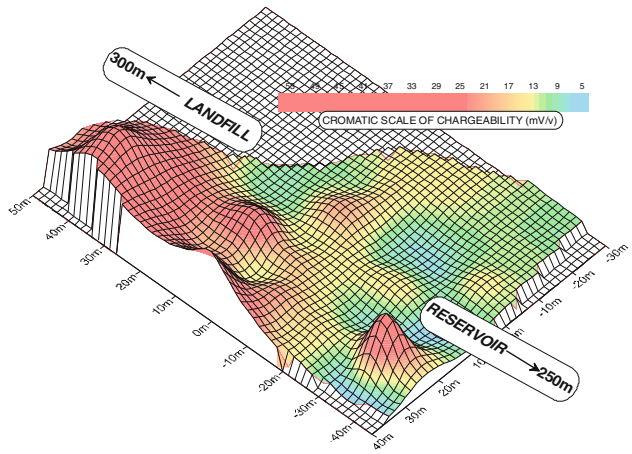

Fig. 10 3D simulation of the modeled chargeability at level 4 of the dipole–dipole

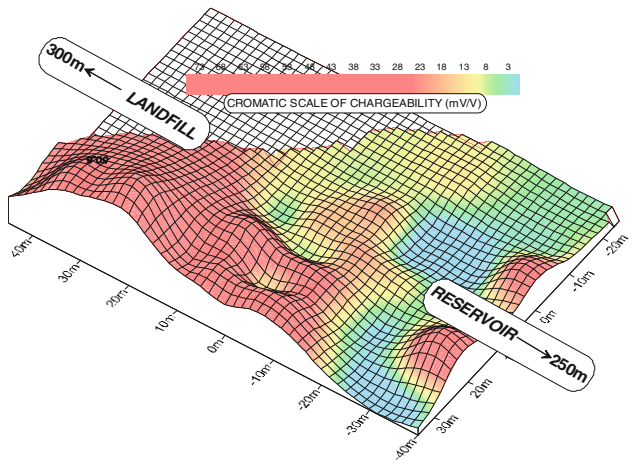

Fig. 11 3D simulation of the modeled chargeability at level 5 of the dipole–dipole

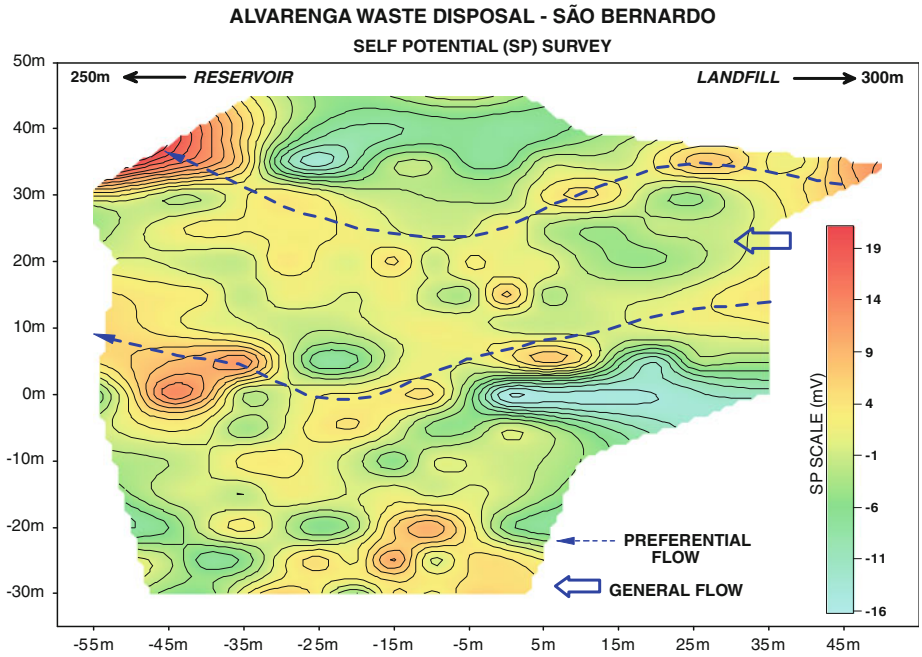

Fig. 12 SP map

In this portion (yellow and red colors = positive values), it is possible to define two flow lines separated by negative values of SP.

Discussion and conclusions

The survey results show that SP, resistivity, and IP methods are excellent tools for surveying contaminated areas; these techniques allow precise definition of the area affected by the pollutants, which will help in directing the remediation process. For conditions, such as those present in the studied area, the potentials generated by the underground fluid flow are the main ones responsible for the natural electrical potentials. Because these potentials are caused by the fluid flow, the electrical potentials increase from upstream to downstream and their amplitudes are proportional to the hydraulic gradient; in other words, the flow direction is from lower to higher electrical potential. This is clear in the SP isopotential map, which shows the preferable flow directions (Fig. 12). In addition, SP is a very simple, fast and low cost method.

The resistivity results clearly show that the lower resistivity zones are the areas most contaminated by the leakage, which is in agreement with Elis (1999), Gallas et al. (2003), Silva (2003) and Soupios et al. (2007). The higher resistivities are related to deeper levels that have not yet been reached by the leakage plume. In the downstream region, low resistivities appear even in the deepest levels, suggesting more intense penetration of the contamination plume in that locale.

The behavior of the IP parameter is similar to that exhibited by the resistivity data. Lower values of chargeability are related to the more superficial levels where the contamination is more intense. Therefore, the IP phenomenon is clearly inversely proportional to the ion content, as demonstrated by Eqs. 5 and 6 and Gallas (2000). Therefore, lower resistivity in the contaminated area is related to higher ion concentration in the phreatic electrolyte, which favors electrical ionic conduction. It was also possible to confirm that higher ionic concentration is inversely proportional to the IP effect.

It is important to note that even though the IP data identified the contaminated zones, resistivity exhibited a better correlation with the presence of contamination. It is possible that the IP method may yield better results in other geological contexts or even with other types of contaminants. A limitation of its use, however, is its relatively higher cost, which is due in part to the greater time required to acquire data in the field.

References

Archie GE (1942) The electrical resistivity log as an aid in determining some reservoir characteristics. Trans AIME 146:54–64

Bertin J, Loeb J (1976) Experimental and theoretical aspects of induced polarization. Gebruder Borntraeger, v.1. Geopublication Associates, Berlin-Stuttgart, p 250

Cole KS, Cole RH (1941) Dispersion and absorption in dielectrics. 1 Alternating current fields. J Chem Phys 9:341

deGroot-Hedlin C, Constable S (1990) Occam's inversion to generate smooth, two-dimensional models form magnetotelluric data. Geophysics 55(12):1613–1624

Edwards LS (1977) A modified pseudosection for resistivity and induced-polarization. Geophysics 42(5):1020–1036

Elis VR (1999) Avaliação da aplicabilidade de métodos elétricos de prospecção geofísica no estudo de áreas utilizadas para disposição de resíduos. Tese de Doutorado, Instituto de Geociências e Ciências Exatas, Universidade Estadual Paulista, Rio Claro, p 264

Gallas JDF (2000) Principais métodos geoelétricos e suas aplicações em prospecção mineral, hidrogeologia, geologia de engenharia e geologia ambiental. Tese de Doutorado, Instituto de Geociências e Ciências Exatas, Universidade Estadual Paulista, Rio Claro, p 174

Gallas JDF, Malagutti Filho W (2001) O método do potencial espontâneo (SP) na detecção de infiltrações em barragens. In: Anais (CD-ROM) Congresso Internacional da Sociedade Brasileira de Geofísica, Salvador

Gallas JDF, Malagutti Filho W, Prado RL, Taioli F (2003) Lixão do Alvarenga—Mapeamento da pluma de contaminação pelos métodos geoelétricos. In: Anais CD-ROM Congresso Internacional da Sociedade Brasileira de Geofísica, Rio de Janeiro

Godio A, Naldi M (2003) Two-dimensional electrical imaging for detection of hydrocarbon contaminants. Eur Assoc Geosci Eng Near Surf Geophys 1:131–137

Grahame SA (1947) The electrical double layer and the theory of electrocapillarity. Chem Rev 41:441–501

Hallof PG (1957) On the interpretation of resistivity and induced polarization measurements. PhD Thesis, MIT

Keller GV, Frischknecht FC (1977) Electrical methods in geophysical prospecting. Pergamon Press, Oxford, p 517

Klein JD, Shuey RT (1978a) Nonlinear impedance of mineral-electrolyte interface: Part I. Pyrite. Geophysics 43(6):1222–1234

Klein JD, Shuey RT (1978b) Nonlinear impedance of mineral-electrolyte interface: Part II. Galena, chalcopyrite, and graphite. Geophysics 43(6):1235–1249

Loke MH, Barker RD (1996a) Rapid least-squares inversion of apparent resistivity pseudosections by a quasi-Newton method. Geophys Prospect 44(1):131–152

Loke MH, Barker RD (1996b) Practical techniques for 3D resistivity surveys and data inversion. Geophys Prospect 44(3):499–523

Nascimento CTC, Koide S, Pires ACB, Mello GA (1999) Pseudo-seções elétricas na avaliação da contaminação do subsolo. Revista Brasileira de Geociências 29(4):621–626

Ogilvy R, Meldrum P, Chambers J, Williams G (2002) The use of 3D electrical resistivity tomography to characterize waste and leachate distribution within a closed landfill, Thriplow, UK. J Environ Eng Geophys 7(1):11–18

Orellana E (1972) Prospeccion geoeletrica en corriente continua. Paraninfo, Madrid, p 523

RES2DINV ver. 3.54 (2004) Rapid 2-D resistivity and IP inversion using the least-squares method. Geoelectric Imaging 2-D and 3D. Geotomo Software, Malaysia

Roy KK, Elliot HM (1980) Model studies on some aspects of resistivity and membrane polarization behavior over a layered earth. Geophys Prospect 28(5):759–775

Seaton WJ, Burbey TJ (2002) Evaluation of two-dimensional resistivity methods in a fractured crystalline–rock terrane. J Appl Geophys 51:21–41

Silva JTC (2003) Métodos geoelétricos em apoio ao mapeamento de contaminação por esgotos domésticos em Salesópolis, SP. Trabalho de formatura, Instituto de Geociências, Universidade de São Paulo, São Paulo, p 39

Soupios P, Papadopoulos N, Papadopoulos I, Valianatos F, Sarris A, Manios T (2007) Application of integrated methods in mapping waste disposal areas. Environ Geol 53(1):661–675

Sumner JS (1976) Principles of induced polarization for geophysical exploration. Elsevier Scientific Publishing Co, New York, p 277

Telford WM, Geldart LP, Sheriff RE (1990) Applied geophysics, 2nd edn. Cambridge University Press, Cambridge, p 770

Varnier C, Hirata R (2002) Contaminação da água subterrânea por nitrato no Parque Ecológico do Tietê–São Paulo, Brasil. Revista Águas Subterrâneas 16:77–82

Vega de la M, Osella A, Lascano E (2003) Joint inversion of Wenner and dipole–dipole data to study a gasoline-contaminated soil. J Appl Geophys 54:97–109

Ward SH (1990) Resistivity and induced polarization methods. Geotechnical and Environmental Geophysics. Society of Exploration Geophysicists, v.1: Review and Tutorial, pp 147–189